International Journal of Science and Research (IJSR)
ISSN (Online): 2319-7064
Index Copernicus Value (2013): 6.14 | Impact Factor (2014): 5.611

Studies on Physical and Electrical Characterization of Al_2O_3-ZnO Composite Material and its Thick Films

M. K. Deore

Material Research Laboratory, Department of Physics, M. V. P. Samaj's, Arts, Science and Commerce College, Ozar (Mig) 422206, India

Abstract: ***Al_2O_3 - ZnO composite material was obtained by adding the Aluminium chloride ($AlCl_3 \cdot 6H_2O$) (Hexahydrate) powder of different weight percent (0.5, 1 3, 5 and 7 wt %) and Analar Reagent grade (99.9 % pure) ZnO powder by mixing mechnochemically in acetone medium. The prepared materials were sintered at 1000°C for 12h in air ambience and ball milled to ensure sufficiently fine particle size. The structural properties of the powder materials were investigated by X-ray diffraction analysis. The observed powder materials show the polycrystalline nature and the crystallite size found to be in the range of 10 to 36 nm. The thick films of undoped ZnO and Al_2O_3 doped-ZnO were prepared by screen printing technique. The surface morphology of the films was studied by SEM and it shows the films are porous in nature and petal-shaped grains of sizes varies from 190nm to 276nm were observed. The final composition of each film was determined by EDAX analysis.The At. wt. % of Zn and O in each sample was not as per stoichiometric proportion. The electrical conductivity and activation energy of all films were determined.***

Keywords: ZnO, Al_2O_3, Thick Films, Crystalline size, Electrical Conductivity, Activation Energy.

1. Introduction

The requirements of semiconductor material are increased along with the expanding of global electronic industry [1] [2]. Semiconductor metal oxides as high performance catalysts for energetically and environmentally improved catalytic combustion of sulfur and hydrocarbons. In order to enhance the catalytic activity (oxidation), the oxides were doped with it using mechanical mixing of some impurities. The aim of present research work is to enhance the catalytic activity (oxidation) of Zinc Oxide (ZnO) using mechanical mixing of Al_2O_3. Metal oxides are extremely important technological materials for use in electronic and photonic devices. The conventional oxide-mixing techniques; powders are produced more homogeneous after the sintering process. In addition, the grain size obtained is much smaller [3]-[4].

Al_2O_3 is weak n-type semiconductor material with wide band gap(8.8 ev) for bulk material in different crystalline form and good thermal stability. It works as good catalyst with semiconductor when the gases such as H_2S and Ethanol come in contact with it.

Zinc oxide (ZnO) is an n-type direct band semiconductor of a wide bandgap (3.4 eV). It is an important multifunctional material with wide ranging applications in varistors [5],surface acoustic wave (SAW) devices[6], transparent conducting oxide electrodes [7], solar cells [8], blue/UV light emitting devices [9], gas sensors [10]-[11], etc. Its conductivity can be tailored by controlling the deviation from stoichiometry and by doping [12]. The undoped -ZnO has high n-type conductivity due to defects such as oxygen vacancies and Zn interstitials, which form donor levels [13]. Group IIIa elements (Al, Ga, In) have been used to improve the electrical conductivity and thermal stability of ZnO films. For this work, Al^{3+} substitution on Zn^{2+}(was chosen due to the small ion size of Al^{3+} compared to that of Zn^{2+}(Al^{3+} (0.53Å) and Zn^{2+} (0.74 Å)).

2. Experimental Procedure

2.1 Preparation of Functional Material

Al_2O_3 - ZnO composite material were obtained by adding the Aluminium chloride ($AlCl_3 \cdot 6H_2O$) (Hexahydrate) powder of different weight percent (0.5, 1 3, 5 and 7 wt %) and Analar Reagent grade (99.9 % pure) ZnO powder by mixing mechnochemically in acetone medium. The prepared materials were sintered at 1000°C for 12h in air ambience and ball milled to ensure sufficiently fine particle size.

2.2. Preparation of Thick Films

The thixotropic paste was formulated by mixing the fine powder of functional material with a solution of ethyl cellulose (a temporary binder) [14] in a mixture of organic solvents such as butyl cellulose, butyl carbitol acetate and terpineol, etc. The ratio of the inorganic to organic part was kept at 75:25 in formulating the paste. This paste was screen-printed [15]-[16] on a glass substrate in a desired pattern (1.5cm x 0.5cm). The films were fired at 550°C for 30 min. in air atmosphere

.

2.3. Thickness measurements of films

The range of thicknesses of the films was observed in the range from 55 to 65µm. The reproducibility in thickness of the films was possible by maintaining the proper rheology and thixotropy of the paste.

3. Physical Characterization

3.1. Structural analysis

In order to understand the structural properties of AlO_3 - doped ZnO powder materials at different dopant concentration, X-ray diffraction analysis of these sintered

powders were carried out in the 20-80^0 range using Cuk$_\alpha$ radiation.

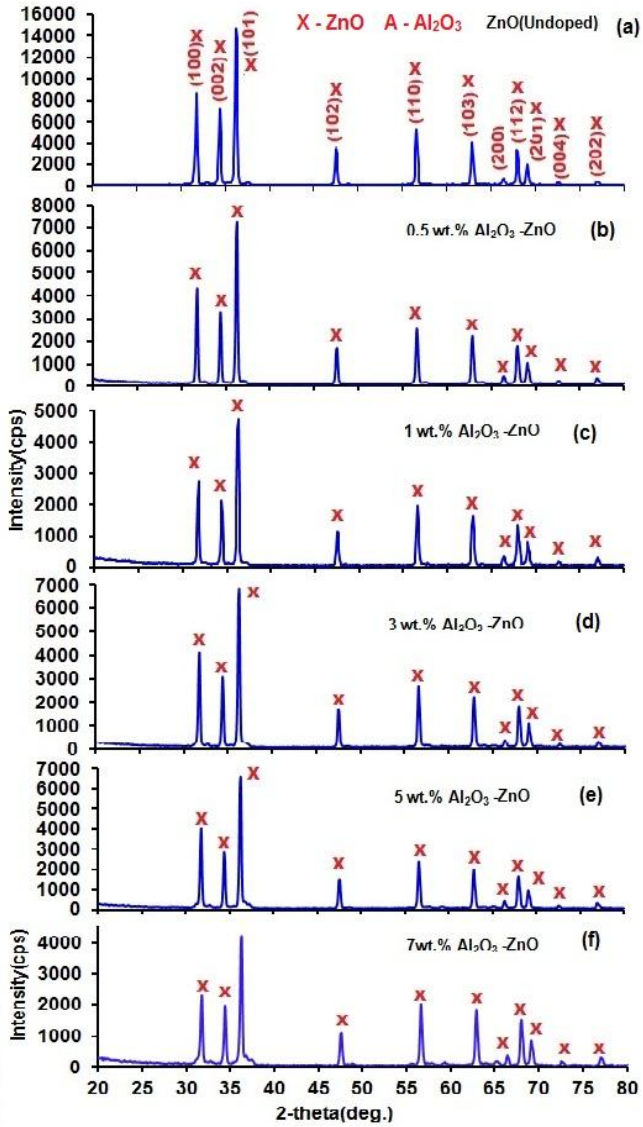

Figure 1: XRD pattern of undoped ZnO and Al_2O_3-ZnO composite material

Figs.1 (a - f) shows XRD patterns of undoped- ZnO, Al_2O_3 and Al_2O_3-ZnO (0.5, 1, 3, 5 and 7 wt. %). Fig.1 (a) shows XRD patterns of ZnO material. The observed diffraction peaks of ZnO are corresponding to the hexagonal wurtzite structure of ZnO. The observed peaks are well matched with the JCPDS (76-0704) reported data of ZnO. The sharp peaks of XRD are corresponds to ZnO material and are observed to be polycrystalline in nature. The higher peak intensities of an XRD pattern is due to the better crystallinity with preferred orientation along the (101) direction.

Figs. 1(b-f) show the XRD patterns of 0.5, 1, 3.5, and 7 wt. % Al_2O_3-ZnO. For all the compositions, formation of only ZnO wurtzite phase is observed in accordance with the reported d-values (JCPDS 76-0704). In corresponding XRD data of such materials, the observed diffraction peaks correspond to the hexagonal wurtzite structure of ZnO (JCPDS 76-0704). The higher peak intensities of an XRD pattern are due to the better crystallinity.

Fig.1 shows the XRD spectra of Al_2O_3-doped ZnO composite material. All the patterns exhibit an intensive (002) XRD peak, indicating that they have c-axis-preferred orientation due to the self-texturing mechanism as discussed by Deng et al [23]. The 2θ values of the diffraction peaks (002) are located at 34.40°, which are very close to that of standard ZnO crystal. No Al_2O_3 or $ZnAl_2O_4$ phase was detected from the XRD spectra. This may be due to aluminum replacing zinc substitutionally in the hexagonal lattice or aluminum segregating to the noncrystalline region in grain boundary.

From the XRD results, it is concluded that the material properties are strongly dependent on aluminum concentration. The diffraction peak intensity of Al_2O_3:ZnO films decreased with increased doping concentrations. This indicates that an increase in doping concentration deteriorates the crystallinity of the films, which may be due to the formation of the stresses by the difference in ion sizes between zinc and the dopant [17, 18] and the segregation of dopants in grain boundaries for high doping concentrations.

The average crystallite size was calculated from XRD pattern using Debye Scherer's formula [19].

$$D = \frac{0.9\,\lambda}{\beta\ \mathrm{Cos}\ \theta} \qquad (1)$$

Where D- is average crystallite size,
β - is the broadening of the diffraction line measured at half maximum intensity(FWHM),
λ -is wavelength of the x- ray radiation and (0.1542 nm).
θ - is the Bragg angle

Table 1: XRD data of of undoped ZnO and Al_2O_3-ZnO composite material

Sample	*Sr. No.*	*2θ deg.*	*d-(Å)*	*FWHM*	*D(nm)*	*Plane (hkl)*
Undoped ZnO	1	31.70	2.82	0.265	35	Z-100
	2	72.60	1.30	0.427	26	Z-004
0.5 wt.% Al_2O_3-ZnO	1	31.80	2.81	0.259	35	Z-100
	2	72.60	1.29	1.112	10	Z-004
1 wt.% Al_2O_3-ZnO	1	31.80	2.80	0.258	36	Z-100
	2	72.60	1.30	0.584	19	Z-004
3 wt.% Al_2O_3-ZnO	1	31.80	2.81	0.259	35	Z-100
	2	72.60	1.30	0.611	18	Z-004
5 wt.% Al_2O_3-ZnO	1	31.80	2.80	0.259	35	Z-100
	2	72.60	1.30	1.112	10	Z-004
7 wt.% Al_2O_3-ZnO	1	31.80	2.81	0.259	35	Z-100
	2	72.60	1.298	1.112	10	Z-004

d = Interplaner distance in Å
D = Crystallite Size in nm

Table 1 shows the variation of crystallite size with doping concentration of Al_2O_3 in ZnO samples. Slightly broadening of diffraction lines may be attributed to small crystalline effects [20]. From the XRD pattern, the lattice constants of hexagonal ZnO phase can be calculated using the equation [20]-[21].

$$\frac{1}{d^2_{(hkl)}} = \left(\frac{4}{3}\right) \times \left(\frac{(h^2+hk+k^2)}{a^2}\right) + \left(\frac{l^2}{c^2}\right) \qquad (2)$$

$$\frac{c}{a} = \sqrt{\frac{8}{3}} \quad (3)$$

Where d - is interplanar distance,
a and c - are lattice constants (hexagonal structure)

Table 2: Lattice constants Al_2O_3 -doped ZnO composite material

Phase	*hkl-Plane*	*2θ*	*d (Å)*	*a (Å)*	*c (Å)*
ZnO (Undoped)	101	36.20	2.4794	3.240	5.291
0.5 wt.% Al_2O_3-ZnO	101	36.20	2.4720	3.231	5.276
1 wt.% Al_2O_3-ZnO	101	36.20	2.4688	3.226	5.269
3 wt.% Al_2O_3-ZnO	101	36.20	2.4753	3.235	5.283
5 wt.% Al_2O_3-ZnO	101	36.20	2.4720	3.231	5.276
7 wt.% Al_2O_3-ZnO	101	36.20	2.4720	3.231	5.276

From Table 2, it has been observed that there is variation of lattice constants from JCPDS value (a = 3.253Å, c = 5.213Å). The ionic radius of Zn^{2+} is 0.74Å and of Al^{3+} is 0.53Å [22]. This should result in decreased lattice parameters as per Vegards Law. However, such a trend is not observed as the sintering temperature is very low, and hence diffusion of Al into Zn sites might not have occurred to a complete extent. The possible formation of Al_2O_3 or $ZnAl_2O_4$ phases was not detected. This might be due to relatively low sintering temperature (~1000°C) at which their crystallization might not have occurred, suggesting formation of the secondary phases probably in the amorphous form.

3.2. Micro structural analysis of the films

The surface morphology and chemical composition of the films were analyzed using a scanning electron microscope [SEM model JEOL 6300 (LA) Germany] coupled with an energy dispersive X-ray analysis. (EDAX, JEOL, JED-2300, Germany). Figs. 2 (a-e) show the surface morphology of thick films of pure ZnO and Al_2O_3-ZnO (0.5, 1, 3.5, and 7 wt. %) thick films. Plane-view SEM investigation reveals a porous structure of the ZnO films with different Al_2O_3 doping concentrations. Petal-shaped grains of various sizes were observed in all samples. The grains of sizes varies from 190nm to 276nm. The majority of these grains appear several times larger than the average crystallite sizes calculated from X-ray diffraction data (10-36 nm) thus, indicating that most of the grains comprise multiple crystallites. No systematic variation in the microstructure of the ZnO films as a function of the doping concentration was detected.

The ZnO film doped with 1 wt. % Al_2O_3 was observed to be the most porous. The Al_2O_3 additives would present on the ZnO grains are in an optimum level leading to high porosity..

In Figs.2 (d, e and f), the Al_2O_3 additives distributed on ZnO grains would be greater than optimum level, it reduces the porosity of the film surface.

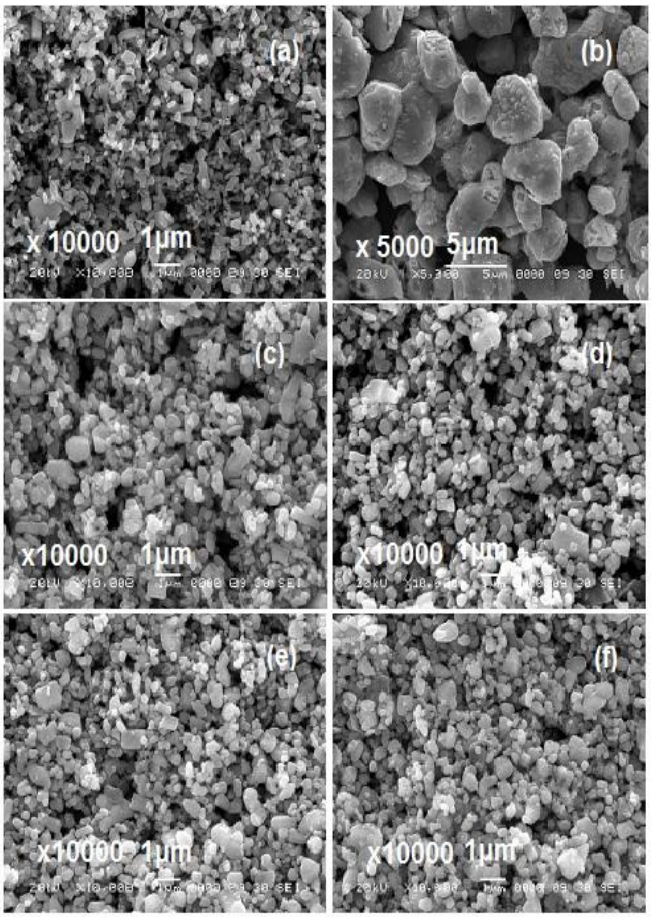

Figure 2: SEM images of (a) undoped ZnO, (b) 0.5 wt.% (c)1 wt.% (d) 3 wt.% (e) 5 wt.% and (f) 7 wt.% Al_2O_3 – ZnO films

.

3.3 Elemental analysis of the films

The composition of pure and Al_2O_3 -doped ZnO thick films with different mass ratio were analyzed by energy dispersive X-ray analysis. ((EDAX, 6360LA).

Table 3: Quantative elemental analysis of undoped ZnO and Al_2O_3 - ZnO films

Sample	*At. Wt. % of Elements*			
	O	*Zn*	*Al*	*Total*
ZnO (Undoped)	21.18	78.82	-	100
0.5 wt.% Al_2O_3-ZnO	16.71	83.44	0.35	100
1 wt.% Al_2O_3-ZnO	15.43	83.45	2.12	100
3 wt.% Al_2O_3-ZnO	17.25	80.22	2.53	100
5 wt.% Al_2O_3-ZnO	18.31	77.83	3.86	100
7 wt.% Al_2O_3-ZnO	18.44	76.28	5.27	100

Table.3 gives quantitative elemental analysis of Al_2O_3 - doped ZnO thick films at different level. The EDAX analysis shows presence of only Zn, Al and O as expected, no other impurity elements were present in the thick films. The EDAX result shows variation in Zn/O ratio and Al/Zn ratio with variation in doping concentration. The At. wt. % of Zn and O in each sample was not as per stoichiometric proportion. The entire samples were observed to be oxygen deficient.

4. Electrical Characterization

4.1 I-V Characteristics of the films

Fig. 3 shows the I-V characteristics of pure and Al_2O_3 doped ZnO films at room temperature in air ambience. I-V Characteristics are observed to be symmetrical in nature, indicating the ohmic nature of aluminium contacts.

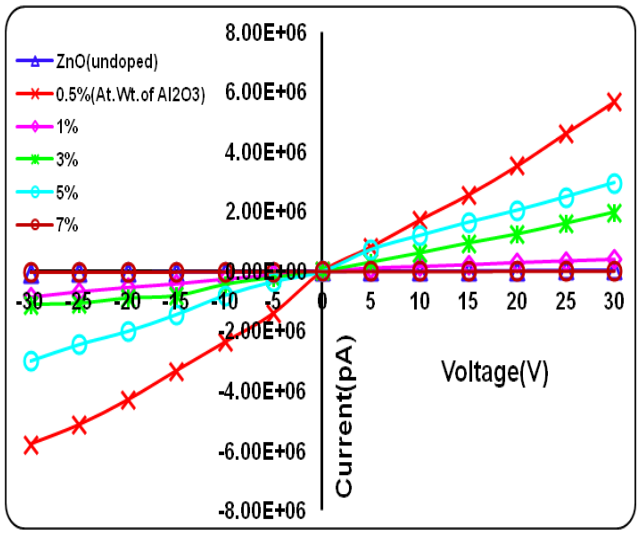

Figure 3: I-V characteristics of undoped and Al_2O_3 - ZnO films at room temperature

4.2. Electrical conductivity of the films

The conductivity of Al_2O_3 -doped ZnO thick films at constant temperature was calculated using the Eq. (4)[23],

$$\sigma = \frac{l}{(R*b*t)}\left(\frac{1}{\Omega - m}\right) \quad (4)$$

Where
R = Resistance of thick film at constant temperature
t = thickness of the film sample
l = length of the thick film
b = breadth of the thick film

Fig.4 shows that the conductivity films increases with increase in dopant concentration of Al_2O_3 up to 3 wt. % then decreases with increase in dopant concentration of Al_2O_3 i.e from 5 wt. % to 7 wt. %. Thus, it was found that the conductivity of Al_2O_3- ZnO films is strongly dependent on the Al_2O_3 dopant concentration. In general, at low doping concentration of i.e. below the solubility limit, Al^{3+} ions substitute Zn^{2+} ions in the ZnO lattice site and increase the electrical conductivity by increasing the donor

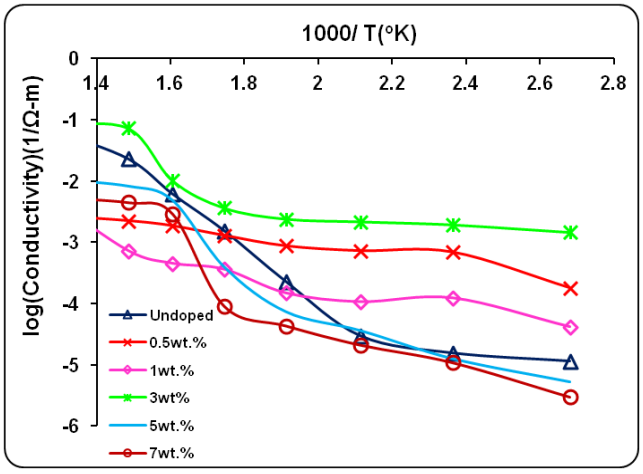

Figure 4: Conductivity –Temperature profile of undoped and Al_2O_3 - ZnO films

concentration [24] – [26]. These reactions easily take place because Al^{3+} (0.53Å) and Zn^{2+} (0.74 Å) have similar ionic radii.

$$Al_2O_3 + ZnO \rightarrow Zn_{Zn} + 2Al^{\bullet}_{Zn} + 3O_o^{x} + \tfrac{1}{2}\, O_{2(g)} + 2e^{-} \quad (5)$$

Where 0_o^x is the oxygen at oxygen site

At high doping concentration Al atoms may also enter the structure and have preference for interstitial sites. This interstitial substitution occurs either directly or by substitution of Zn atoms on its regular site at first and then moving to the interstitial position. At the interstitial position, the aluminium atoms absorb an electron. In this case, the aluminium behaves as an acceptor and decreases the conductivity [27].

$$Al_2O_3 + ZnO \rightarrow Zn_{Zn} + 2Al^{\bullet}_{Zn} + 3O_o^{x} + O_i'' \quad (6)$$

Where O_i'' is the negatively charged oxygen interstitial, 0_o^x the oxygen at oxygen site,

Eq. (5) indicates a decrease in resistance whereas Eq. (6) lead to an increase in resistance. It may be concluded from Fig. 4 that in the present sample Eq. (6) is predominantly operative for undoped and 0.5, 1, 3 wt. % Al_2O_3 doped ZnO, indicating an increase in conductivity, and the mechanism from Eq.(6) is possibly favorable at higher dopant concentrations of Al_2O_3 (5, 7 wt. %) in indicating decrease in conductivity.

4.3. Activation energy of the films

Activation energy can be thought of as the height of the potential barrier or energy barrier separating two minima of potential energy. Activation energy of Al_2O_3 doped ZnO thick films were calculated from Arrhenius plot for different operating temperature regions by using Eq. (7).[28]

$$\sigma = \sigma_o e^{-\Delta E/KT} \quad (7)$$

Where
σ = Electrical conductivity $(\Omega\ cm)^{-1}$
σ_o = Electrical conductivity at const. temp.$(\Omega\ cm)^{-1}$
ΔE = Activation energy of the electron transport in the conduction band,
K = Boltzmann constant, T = Absolute temperature.

Table 7.4: Activation energy of undoped and Al_2O_3 -ZnO film with temperature

T(°C)	Activation energy (ev)					
	Undoped	Al_2O_3 -doped ZnO				
	ZnO	0.5wt.%	1%wt.	3%wt.	5%wt.	7wt%
100	0.032	0.076	0.031	0.007	0.067	0.028
150	0.028	0.092	0.023	0.005	0.080	0.053
200	0.011	0.094	0.028	0.004	0.078	0.061
250	0.024	0.092	0.026	0.002	0.071	0.071
300	0.064	0.087	0.011	0.005	0.045	0.086
350	0.100	0.070	0.007	0.028	0.004	0.102
400	0.139	0.051	0.003	0.076	0.017	0.116
450	0.177	0.026	0.052	0.086	0.025	0.130

Table 7.4 shows the calculated activation energy of all samples for different doping concentration at different operating temperature regions. Fig. 7.5 shows variation of activation energy of undoped and Al_2O_3 doped ZnO thick films as the function of operating temperature.

The graph shows that the doped film having low activation energy than undoped film. It also shows that the activation energy varies with the dopant concentration. The film doped with 3 wt. % of Al_2O_3 shows lowest activation energy than other doping concentrations. It may be due the barrier height decreases as Al_2O_3 doping increases..

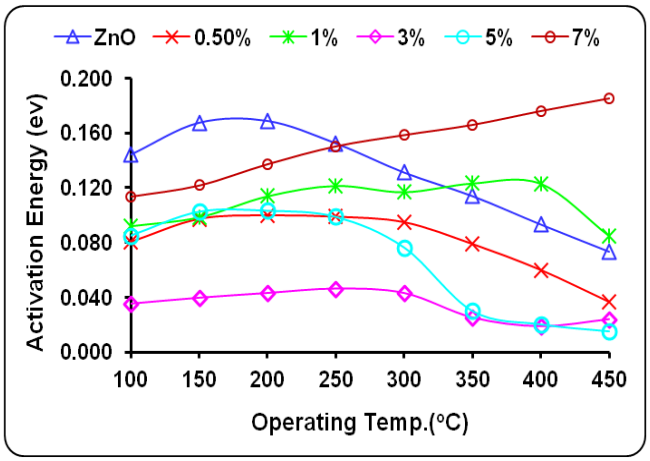

Figure 5: Variation of activation energy with temperature of undoped and Al_2O_3 - ZnO films

5. Summary and Conclusions

From the results obtained, following conclusions can be made

1) It shows that the Al_2O_3 –ZnO functional material can be obtained by mechanochemical method.
2) The XRD analysis shows that the observed powder materials show the polycrystalline nature and the variation in the crystallite size due to doping. The crystallite size was found to be in the range of 10 to 36 nm.
3) The SEM analysis shows the surface morphology of the of undoped ZnO and Al_2O_3 doped-ZnO thick films and it shows the films are porous in nature and petal-shaped grains oriented randomly of sizes varies from 190nm to 276nm were observed.
4) The EDAX analysis shows final composition of each film.The At. wt. % of Zn and O in each sample was not as per stoichiometric proportion. The entire samples were observed to be oxygen deficient.
5) The electrical conductivity for 0.5, 1, 3 wt. % Al_2O_3 doped ZnO increase while at higher dopant concentrations of Al_2O_3 (5, 7 wt. %) it decrease.
6) The doped film shows low activation energy than undoped film. It also shows that the activation energy varies with the dopant concentration. The film doped with 3 wt. % of Al_2O_3 shows lowest activation energy than other doping concentrations. It may be due the barrier height decreases as Al_2O_3 doping increases.
7) Al_2O_3 doped-ZnO thick films would be use full for gas sensing application.

6. Acknowledgment

The author (MKD) is very much thankful to The Sarchitnis, Smt. Nilimatai Pawar, M. V. P. Samaj, Nashik, Dr. V. B. Gaikwad, Director, B.C.U.D. Savitribai Phule Pune University and Dr. A. P. Patil, Principal, Arts, Science and Commerce, College, Ozar (Mig), Dr. G. H. Jain, Principal, Chandwad College for his keen interest in this research.

References

[1] S. Sze, K. N. Kwok, Physics of Semiconductor Devices Wiley Intersccience : New jersey, 2007.
[2] Material Science Outlooks, National Institute for materials Science, Japan, 2005.
[3] E.Y. Gutmanas," Materials with fine microstructures by advanced powder metallurgy". Progr. Mater. Sci. (34), pp. 261–366, 1990.
[4] D. A Porter, K. E. Easterling, Phase Transformations in Metals and Alloys, 2nd ed.; Chapman and Hall: London, UK, 1992.
[5] R.N. Viswanath, S. Ramasamy, R. Ramamoorthy, P. Jayavel, T. Nagarajan, "Preparation and characterization of nanocrystalline ZnO based materials for varistor applications", Nanostruct. Mater. (6),PP. 993–996, 1995.
[6] M.S. Wu, A. Azuma, T. Shiosaki, A. Kawabata, "Low-loss ZnO optical waveguides for SAW-AO applications, IEEE Trans". Ultrasonics Ferroelec.Freq. Control(36),PP. 442–445, 1989.
[7] M.K. Jayaraj, A. Antony, M. Ramachandran, "Transparent conducting zinc oxide thin film prepared by off-axis RF magnetron sputtering", Bull. Mater. Sci.(25),PP. 227–230, 2002.
[8] K. Keis, C. Bauer, G. Boschloo, A. Hagfeldt, K. Westermark, H. Rensmo, H. Siegbahn, "Nanostructured ZnO electrodes for dye-sensitized solar cell applications", J. Photochem. Photobiol. A: Chem. (148) PP. 57–64, 2002.
[9] P. Yang, H. Yan, S. Mao, R. Russo, J. Johnson, R. Saykally, N. Morris, J. Pham, R. He, H. Choi, "Controlled growth of ZnO nanowires and their optical properties", Adv. Funct. Mater. (12),PP. 323–331, 2002.
[10] S. Roy, S. Basu, "Improved zinc oxide film for gas sensor applications", Bull. Mater. Sci. (25),PP.513–515, 2002.

[11] A.R. Raju, C.N.R. Rao, "Gas sensing characteristics of ZnO and copper impregnated ZnO', Sens. Actuators B (3),PP. 305–310, 1991.
[12] J.J. Lander, "Reactions of lithium as a donor and acceptor in ZnO", J. Phys.Chem. Solids (15),PP. 324, 1960.
[13] Look D C, Hemsky J W, Sizelove J R. "Residual Native Shallow Donor in ZnO". Phys. Rev. Lett.,(82),PP. 2552-2555, 1999.
[14] V. B. Gaikwad, S. D. Shinde, D. D. Kajale, Y. R. Baste, P. K. Khanna, N. K. Pawar, D. N. Chavan, M. K. Deore, G. H. Jain, "Studies on Gas Sensing Performance of Pure and Surface Modified SrTiO3 Thick Film Resistors", Sensors and Transducers, (6),PP. 57-68, 2009.
[15] M. K. Deore; G.H. Jain, "Synthesis, characterisation and gas sensing application of nano ZnO material" Int. J. of Nanoparticles, Vol.(7), No.1, pp.57 – 72, 2014 .
[16] D. R. Patil, L. A. Patil, G. H.Jain,M.S. Wagh, S. A. Patil, "Surface activated ZnO thick film resistors for LPG gas sensing", Sensors & Transducers, (74), 874-663, 2006.
[17] A El Hichou, M. Addou, A. Bougrine, R. Dounia, J. Ebothe, M. Troyon, and M. Amrani, "Cathodoluminescence properties of undoped and Al-doped ZnO films deposited on glass substrate by spray pyrolysis". Mat. Chem. Phys., (83)PP. 43-47, 2004.
[18] F. K. Allah, S. Y.Abe, C. M. Nunes, A. Khelil, L.Cattin, M. Morsli, J. C. Bernede, A.Bougrine, M. A. del Valle and F. R. Diaz, "Characterisation of porous doped ZnO thin films deposited by spray pyrolysis technique". Applied Surface Science(253), PP. 9241-9247, 2007.
[19] B. D. Cullity, Elements of X-ray Diffractions, Addison-Wesley, Reading, MA, 1978.
[20] H.P. Klug, L.E. Alexander, X-Ray Diffraction Procedures for Polycrystalline and Amorphous Materials, Wiley, New York, 1974.
[21] M. K. Deore, "Physical, Electrical Properties and Gas Sensing Performance of Pure and NiO-Modified ZnO Thick Films" Sensor Letters, Volume (11), Number 10, pp. 1919-1924, 2013.
[22] K.-C. Hsiao, S.-C. Liao, Y.-J. Che, "Synthesis, characterization and photocatalytic property of nanostructured Al-doped ZnO powders prepared by spray pyrolysis", Mater. Sci. Eng. A 447, PP. 71–76, 2007.
[23] A. S. Garde, "Electrical and Structural Properties of WO3-SnO2 Thick-Film resistors Prepared by Screen Printing Technique",Research Journal of Recent Sciences ,Vol. 4(1), PP. 55-61, January 2015
[24] K.F. Cai, E. Müller, C. Drašar, A. Mrotzek, "Preparation and thermoelectric properties of Al-doped ZnO ceramics". Materials Science and Engineering B(104), pp. 45–48, 2003.
[25] Y. Zhang, and J. Han, "Microstructure and temperature coefficient of resistivity for ZnO ceramics doped with Al_2O_3", Mater. Lett. vol. 60(20) pp. 2522-2525, 2006.
[26] V. Musat, B. Teixeira, E. Fortunato and R. C. C. Monteiro, 2006, "Effect of Post-Heat Treatment on the Electrical and Optical Properties of ZnO:Al thin films", Thin Solid Films, (502),PP. 219- 222, 2006.
[27] J. Han, P. Q. Mantas, and A. M. R. Senos, "Effect of A1 and Mn doping on the electrical conductivity of ZnO," Journal of the European Ceramic Society, vol. 21, no. 10-11, pp. 1883–1886, 2001.
[28] S. Varghese and Mercy Iype, "Effect of Annealing on the Activation Energy of Thin Films of Manganese Sulphide, Copper Phthalocyanine and Multilayer Manganese Sulphide-Copper Phthalocyanine from their Electrical Studies", Oriental Journal of Chemistry Vol. (27), No. (1),PP. 265-269, 2011.

Author Profile

M. K. Deore (India) is Associate Professor of Physics at M. V. P. Samaj's, Arts, Science and Commerce, College, Ozar (Mig), India. He received his M. Sc. degree in Physics in 1988 and Ph. D. degree in 2012 from the Savitribai Phule Pune University, Pune, India; He is working on metal oxide semiconductor gas sensor and nano materials.